NeuroImage 266 (2023) 119832

Contents lists available at ScienceDirect

NeuroImage

journal homepage: www.elsevier.com/locate/neuroimage

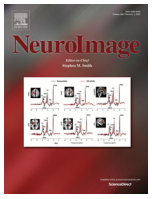

Modulation of pulvinar connectivity with cortical areas in the control of selective visual attention

Carole Guedj*, Patrik Vuilleumier

Neuroscience Department, Laboratory for Behavioral Neurology and Imaging of Cognition, Faculty of Medicine, University of Geneva, Campus BIOTECH H8, 9 Chemin des Mines, Geneva 1202, Switzerland

ARTICLE INFO

Keywords:
Pulvinar
Selective attention
Fronto-parietal attention network
Thalamo-cortical circuit
BetaSeries correlation
Dynamic causal modelling

ABSTRACT

Selective attention mechanisms operate across large-scale cortical networks by amplifying behaviorally relevant sensory information while suppressing interference from distractors. Although it is known that fronto-parietal regions convey information about attentional priorities, it is unclear how such cortical communication is orchestrated. Based on its unique connectivity pattern with the cortex, we hypothesized that the pulvinar, a nucleus of the thalamus, may play a key role in coordinating and modulating remote cortical activity during selective attention. By using a visual task that orthogonally manipulated top-down selection and bottom-up competition during functional MRI, we investigated the modulations induced by task-relevant (spatial cue) and task-irrelevant but salient (distractor) stimuli on functional interactions between the pulvinar, occipito-temporal cortex, and frontoparietal areas involved in selective attention. Pulvinar activity and connectivity were distinctively modulated during the co-occurrence of the cue and salient distractor stimuli, as opposed to the presence of one of these factors alone. Causal modelling analysis further indicated that the pulvinar acted by weighting excitatory signals to cortical areas, predominantly in the presence of both the cue and the distractor. These results converge to support a pivotal role of the pulvinar in integrating top-down and bottom-up signals among distributed networks when confronted with conflicting visual stimuli, and thus contributing to shape priority maps for the guidance of attention.

1. Introduction

The pulvinar is the largest thalamic nucleus in the primate brain (Chalfin et al., 2007) and it is involved in a number of high-level cognitive processes. It has an extensive range of reciprocal connections to virtually the entire neocortex and many subcortical areas (Kaas and Lyon, 2007; Shipp, 2003), making it well placed to influence information processing throughout the brain. Functionally, the pulvinar has been implicated in several attention processes, such as spatial orienting (Rafal and Posner, 1987), salience detection (Snow et al., 2009), filtering irrelevant but salient visual distractors (Fischer and Whitney, 2012), as well as in emotional (Bertini et al., 2018; Lucas et al., 2019) and even motor processes (Wilke et al., 2018). Using connectivity analysis of resting brain activity (Guedj and Vuilleumier, 2020), we recently demonstrated that the pulvinar is functionally subdivided into five clusters, each associated with a distinct connectivity pattern. Furthermore, our decoding analysis on the clusters' co-activation maps indicated that the pulvinar contributes to different behavioral domains (including not only perception, but also emotion or memory), supporting a central and integrative function in the coordination of cortico-subcortical processes across distributed brain networks (Guedj and Vuilleumier, 2020).

Such integrative ability dovetails with a general role in selective attention control, as suggested by early theoretical models (LaBerge and Buchsbaum, 1990; Mesulam, 1999; Posner and Petersen, 1990). In keeping with this, electrophysiology studies in monkeys found increased responses in pulvinar neurons to spatial cues that direct attention to a location in the visual field in covert attention tasks (Fiebelkorn et al., 2019; Saalmann et al., 2012; Zhou et al., 2016). Furthermore, during selective visual attention, the pulvinar was shown to synchronize neural activity between remote cortical areas such as visual areas V4 and TEO (Cortes et al., 2020; Saalmann et al., 2012), lateral intraparietal area and V4 (Saalmann et al., 2018), or LIP and FEF (Fiebelkorn et al., 2019). Accordingly, we recently proposed that the pulvinar may act to compute attentional priority maps through a modulation of functional interactions taking place among cortical areas (Bourgeois et al., 2020). Selective attention governs conscious perception by amplifying behaviorally relevant sensory information, while suppressing interference from distractors, and acts by coordinating neural activity across distributed brain networks including subcortical nodes in pulvinar (Fischer and Whitney, 2012; Saalmann et al., 2012). The visual scene typically comprises multiple stimuli whose features are extracted by pre-attentive detection mechanisms operating in parallel across the visual field and provid-

* Corresponding author.
E-mail address: caroleguedj@yahoo.fr (C. Guedj).
https://doi.org/10.1016/j.neuroimage.2022.119832.
Received 12 September 2022; Received in revised form 13 December 2022; Accepted 22 December 2022
Available online 23 December 2022.

ing a stimulus-driven prioritization that may lead to attentional capture (Gaspelin and Luck, 2018; Wolfe, 2021). However, visual information processing is further influenced by top-down cognitive factors such as expectation, goals, or memory, ultimately forming a priority map that guides selective attention and visuomotor behavior. Such 'priority' thus implies an integration of both bottom-up stimulus-driven and top-down goal-driven signals in order to focus attention on behaviorally relevant stimuli (Bisley and Goldberg, 2010; Fecteau and Munoz, 2006). Given its unique connectivity pattern, the pulvinar is thought to play a major role in this integration by coordinating remote cortical areas.

To test this hypothesis, in the present study, we designed a simple attentional task where attentional priority is expected to be determined by both a top-down "selection" signal, in the form of a central endogenous cue, and a bottom-up "distraction" signal, in the form of a salient exogeneous stimulus, presented together with a target stimulus in a search display. In this task, participants had to report the presence of an indoor or outdoor target scene while covertly exploring the search display. The target was defined as a singleton image colored in red among a set of black-and-white images, such that it could draw attention effectively without requiring a difficult discrimination task. To manipulate top-down attention, a predictive central cue (arrow) indicated the location of the target on half of the trials, whereas the cue was not informative on the other half. Orthogonally, to manipulate bottom-up capture, a salient distractor (face) was also present on half of the trials, shown simultaneously with the target onset and alongside with other non-target scene images. Abundant research has shown that faces produce robust attentional capture due to highly efficient processing of their shape and social salience (Lavie et al., 2003; Vuilleumier et al., 2001). Furthermore, scene and face images evoke differential brain responses in category-selective visual regions, corresponding to PPA and FFA, respectively (Haxby et al., 2001; Kanwisher et al., 1997). Our two experimental factors (i.e., central cue and distractor) were also expected to modulate activity within well-described cortical networks, namely the dorsal (DAN) and ventral (VAN) attention networks (e.g. Corbetta et al. 2008, Corbetta and Shulman 2002, Vossel et al. 2008), typically involved in orienting visual attention toward peripheral targets. Critically, this task allowed us to investigate functional interactions of the pulvinar (a priori defined) with other regions in the brain, including the DAN and VAN as well as visual cortical areas, and to compare its activity and connectivity pattern across different attentional conditions, while keeping task difficulty low and comparable across conditions.

To this aim, we first assessed activations evoked by the cue and salient distractor stimuli in regions of interest, either functionally or anatomically defined. We focused our analysis on: (1) attentional processing within early visual areas responsive to particular retinotopic locations, (2) stimulus encoding within higher visual areas responsive to scenes and faces, (3) main effects observed in predefined regions of interest (ROIs) in the left and right pulvinar. Second, we examined the modulations induced by task contingencies on functional interactions between the pulvinar, visual areas, and cortical nodes of the DAN and VAN. Finally, we characterized the causal influence of the pulvinar on other regions by using dynamic causal modelling (DCM). Our results reveal selective functional interactions linking the pulvinar with FFA, involved in encoding salient face distractors, and pIPS, a key node of DAN involved in orienting spatial attention, whose coupling is modulated by the different stimulus conditions. In particular, our data suggest that the pulvinar may act by weighting signals from concurrent visual stimuli in order to shape priority maps for the guidance of attention.

2. Methods

2.1. Participants

Thirty right-handed participants with no history of psychological or neurological disease and with normal or corrected vision were included in the analyses (15 females; mean age: 23.47 y; SD: 4.43). Four additional participants were recruited but excluded due to drowsiness during scanning and/or poor performance (i.e. response accuracy <70%). All gave written informed consent. The study was conducted in accordance with the Declaration of Helsinki and approved by the Research Ethics Committee of the Geneva University Hospital (CER 11–250).

2.2. Experimental design and task

2.2.1. Attentional task: main experiment

Each trial started with a black screen and a white fixation cross at the center, surrounded by 6 white squares (eccentricity: 12° of visual angle) corresponding to the location of forthcoming images, shown for 500 ms (Fig. 1). Then, for 200 ms, either a white arrow appeared at screen center, pointing to the location of the upcoming target image ('cue' condition), or a white dot replaced the fixation cross ('no cue' condition). The cue was always valid and present in 50% of trials. Please note that this task design was implemented in order to manipulate the priority representation of concurrent stimuli and therefore did not require uncertainty about the cue (valid vs. invalid) as in a standard Posner task (Coull, 1998; Posner, 1980; Posner and Petersen, 1990). Finally, eight randomized images of indoor/outdoor scenes (size: 7°x7° of visual angle) were displayed around central fixation for 2500 ms, all black-and-white except for one colored in red (alpha-blending at 0.1 with RGB color code [255,0,0]) which was the to-be-reported target. The colored feature of the target stimuli allowed an efficient covert capture into the priority map (Wolfe, 2021).

Participant had to categorize the red target as indoor or outdoor as quickly as possible by clicking on a keypad, while being specifically asked to keep their gaze on the fixation cross for the duration of each trial. Offline analysis of eyetracking data confirmed that the instruction to maintain fixation was well observed by the participants overall (gaze fixation was maintained on central cross for more than 70% of trial duration in 26 out of 30 participants). For the sake of reliability, two analyses described below (VOIs on early visual areas and BSC) were also computed while removing four subjects with poor fixation and similar results were obtained.

In half of the trials, a non-target scene image was replaced by a salient distractor, consisting of a neutral face in front-view (Langton et al., 2008). The target and salient distractor were presented at diagonal locations to avoid overlap in the same hemifield and limit the number of possible configurations. Intertrial Interval (ITI) times ranged randomly between 1000 and 3000 ms. A few longer ITIs (8000 ms) were also introduced (3 times per run) to allow the fMRI signal to return to baseline levels. Each task run comprised 100 trials, and each participant performed 3 runs with randomized sequences.

Face and scene stimuli were used because these images engage distinct category-selective areas in extrastriate visual cortex (Haxby et al., 2001; Kanwisher et al., 1997). Faces were randomly chosen from a pool of 8 images (4 men, 4 women), selected from the Karolinska Directed Emotional Faces database (https://www.kdef.se, Lundqvist et al., 1998) and preprocessed for normalization and equalization of spectrum, histogram, and intensity (SHINE toolbox, Willenbockel et al., 2010). Indoor and outdoor images were chosen from a pool of 10 images (5 indoor, 5 outdoor), selected from the ReCor Database (Peyrin, 2018; osf.io/xjdq4). Image size was 1042 × 768 pixels. All tasks were controlled using the Cogent 2000 MATLAB toolbox.

2.2.2. Position localizer task

To define early retinotopic visual areas responding to the target and salient distractor stimuli locations, we used a flickering checkerboard task in which high-contrast patterns rapidly alternated (from black to white and from white to black) successively appeared at the four possible target or salient distractor positions in the visual field (i.e. each in a different quadrant of the search display: top-left, top-right, bottom-left, bottom-right; 12° of visual angle eccentricity; 10°x10° of visual angle).

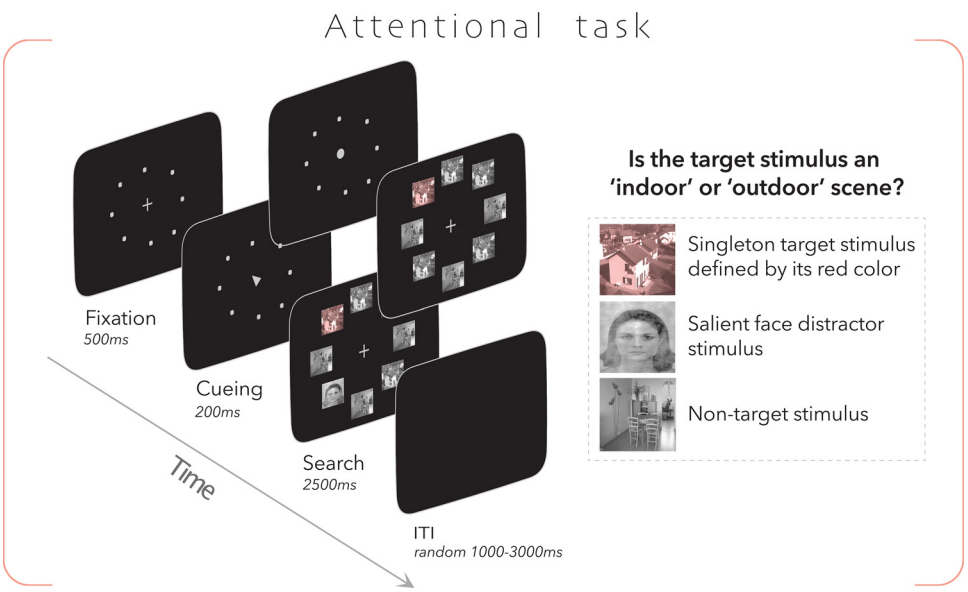

Fig. 1. Attentional task.
Each trial started with a black screen with a fixation cross in the center surrounded by white squares showing the location of forthcoming images. Then, either a white arrow pointing to the location of the upcoming target image (50% of trials) or a white dot (50% of trials) appeared at the center for 200 ms. The arrow cue was always valid. This was followed by a search display with eight scene images equally spaced around fixation, including one singleton colored in red (target). Participants had to categorize the target scene as indoor or outdoor. In half of trials, one of the non-target scene images was replaced by a neutral, task-irrelevant face (salient distractor).

The localizer was divided in five blocks (four quadrants plus an additional condition without any stimulation), where checkerboards were flipped twenty times (each presented for 10 ms with an ITI of 50 ms). Blocks were presented in random order with an inter-block interval of 3 seconds. Participants had to fixate a central white dot on the screen throughout the task and to press a button every time the dot transiently turned red.

2.2.3. Category-selective localizer task

To identify face-responsive and scene-responsive regions in individual brains, single pictures of a neutral face, house, corridor, or scramble image (4 conditions, 10 pictures per condition, all gray-scale, 10°x10° of visual angle) were successively displayed at the 4 possible target locations. In total, 320 stimuli were presented in 8 blocks, each containing 10 pictures of each type at one pseudo-random location. Each picture was shown for 500 ms, with ITI 50 msec. Subjects had to press a button whenever the same stimulus was presented twice in a row. Blocks were presented in random order, with a 3 sec interval.

2.3. fMRI data acquisition

This study was conducted on the imaging platform at the Brain and Behavior Laboratory (BBL) and benefited from support of the BBL technical staff. A 3T TIM Trio System (Siemens, Erlangen, Germany) was used to acquire both high-resolution structural images (MPRAGE, TR = 1900 msec, TE = 2.27 ms, TI = 900 msec, flip angle = 9°, FOV = 256 × 256 mm^2, image matrix 256 × 256, 192 sagittal slices, voxel size = 1 mm isotropic, 32-channel head coil), and T2*-weighted axial echoplanar images (EPIs) with BOLD contrast (GE-EPI, TR = 720 msec, TE = 30.2 msec, flip angle = 52°, FOV = 210 × 210 mm^2, image matrix 84 × 84, 54 sagittal slices, slice thickness = 2.5mm, with a multiband acceleration factor of 6, voxel size = 2.5 mm isotropic, 32-channel head coil). B0 field maps (GR, 2D, TR = 528 msec, short TE = 5.19 msec, long TE = 7.65 msec, flip angle = 60°, FOV = 210 × 210 mm^2, image matrix 84 × 84, negative blip direction, slice thickness = 2.5 mm, 32-channel head coil) were also acquired to correct for static magnetic field inhomogeneities in the EPI images. On average, 786 (±32) volume images were acquired for each run.

2.4. fMRI preprocessing

All preprocessing steps were performed using SPM12 (Wellcome Department of Imaging Neuroscience, London; www.fil.ion.ucl.ac.uk/spm Friston et al., 1994). The first 15 images of functional sequences were removed to allow BOLD signal stabilization. Scans from each subject were realigned using the first as a reference, corrected for B0 field inhomogeneities using phase maps obtained with the SPM12 FieldMap toolbox, and co-registered to individual anatomical images. All images were spatially normalized into MNI space using parameters obtained from the segmentation of anatomical images and spatially smoothed with a Gaussian kernel of 8 mm full-width at half-maximum. The choice of smoothing threshold was backed up by comparing 8 and 4 mm kernels. To do so, we computed spatial SNR (sSNR) of pulvinar seeds to assess signal intensity of subcortical regions in comparison to background noise (both seeds were 4mm radius spheres) [sSNR= (Mean brain tissue intensity) / (Standard Deviation background)]. We found higher sSNR in the smoothed data at 8mm (sSNR=749 ± 391) compared to smoothed data at 4 mm (sSNR=574 ± 282).

2.5. Behavioral data analysis

Performance was examined across the different task contingencies using accuracy (i.e. percentage of correct trials) and reaction times (RTs). For accuracy data, a two-way [Cue x Salient Distractor] repeated-measures of ANOVA was computed (with the 'rstatix' package for R software - R Foundation for Statistical Computing, Vienna, Austria; www.r-project.org). For RT data, error trials (mean 12.3%) as well as trials with RTs faster than 200 msec or slower than 2500 msec (mean 0.8%) were excluded from analysis. Data were submitted to Linear Mixed Models (LMM, with the 'lme4' package for R software; Bates et al., 2015) to assess the effects of cues and salient distractors. We first defined a null model containing the most appropriate random effects (i.e. factors of non-interest with more than three levels). Random effects were introduced sequentially and their effect on model fit (using restricted maximum likelihood criterion) was assessed through Likelihood Ratio Tests (comparing residuals from each model) in order to identify the model with significantly lower deviance, as estimated by a chi-square test (see Supplementary material, Table S1). We then evaluated the effect of Cue and Salient Distractor (using maximum likelihood criterion) as fixed factors with an analysis of variance using the Satterthwaite's approximation method of degrees of freedom.

2.6. fMRI data analysis

2.6.1. Effect of task contingencies in regions of interest

Definition of VOIs.

Position localizer task. We identified four different volumes of interest (VOIs) in early visual cortical areas using the position localizer

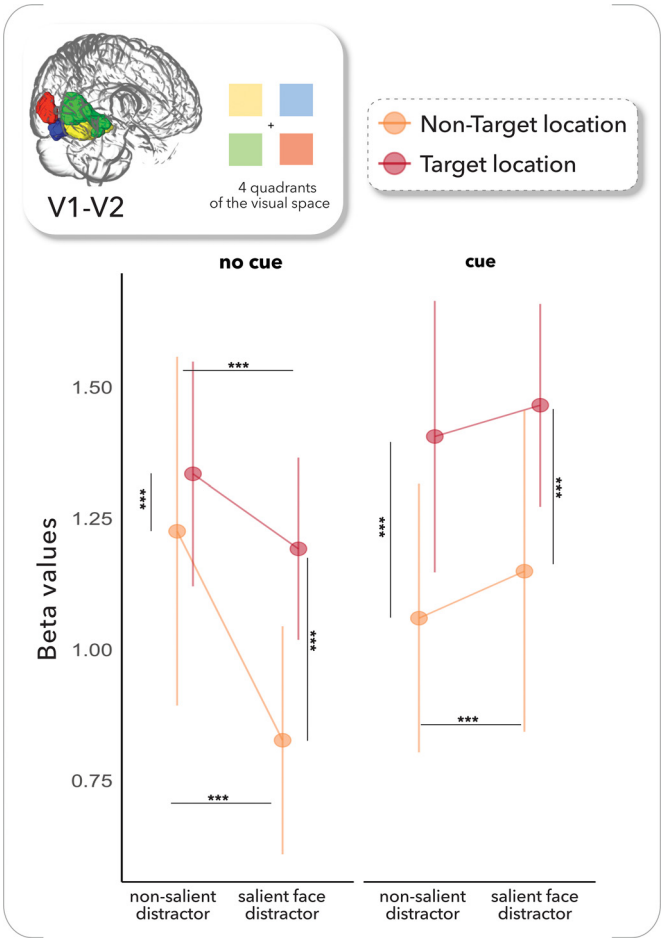

Fig. 2. Attentional modulation of early visual areas by Target and Salient Distractor. Position-specific activation induced by flickering checkerboards in each visual quadrant, projected onto a surface rendering of occipital cortex [top-left insert]. Mean beta values for each position-specific occipital regions (VOIs) across experimental conditions, when the Target is present in the visual quadrant encoded by the respective VOIs versus elsewhere in the display. Error bars reflect the standard errors of the mean (post-hoc tests: ***p-value < 0.001; **p-value < 0.01; *p-value < 0.05).

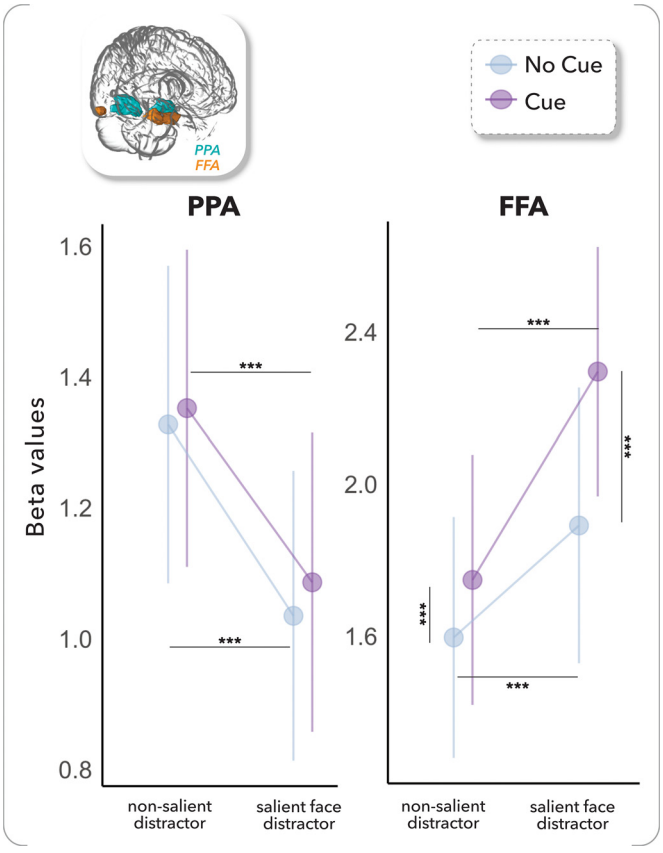

Fig. 3. Visual responses to Target and Salient Distractor stimuli in category-selective visual areas. Brain regions with differential activation to faces (FFA, orange cluster – identified with the localizer task at the group-level: contrast face vs. scene blocks) versus scenes (PPA, cyan cluster – identified with the localizer task at the group-level: contrast scene vs. face blocks) are depicted onto a surface rendering of posterior brain [top-left insert]. Mean beta values are shown for each VOIs according to experimental conditions with different task contingencies. Error bars reflect the standard errors of the mean (post-hoc tests: ***p-value < 0.001; **p-value < 0.01; *p-value < 0.05). Abbreviations: FFA: fusiform face area; PPA: parahippocampal place area.

data, corresponding to the 4 possible areas representing the target or distractor location. Four regressors indicating the onset of stimuli (duration = 6 sec) at the 4 different positions of the localizer task were defined, plus an additional regressor for the period without stimulation. The six parameter estimates for head motion, their derivatives, and the cerebrospinal fluid and white-matter signals (using an erode mask from the segmentation step) were also included as nuisance covariates. The hemodynamic response for each regressor was modeled using a canonical hemodynamic response function in SPM12. In the first level analysis, we contrasted each of the position onset regressors with the other three positions. These contrasts were then taken to the second level analysis to implement a one-sample Analysis Of Variance (ANOVA). We applied a statistical threshold of $p < 0.05$, corrected for multiple comparisons using family-wise error (FWE) correction at the peak level. This allowed us to delineate four distinct regions in early visual cortex responding to the visual locations of Salient Distractors or Targets within the search display (Fig. 2 upper-left insert). These regions overlapped with areas V1 and V2, both known to encode retinotopically specific salience (e.g. Müller and Ebeling 2008, Somers et al. 1999). We then created four spherical VOIs (6 mm radius spheres), centered on the group-based activation peaks, and used them for further analyses of sensory-driven responses in the attentional task.

Category-selective localizer task. We also identified individual VOIs responding to houses and faces stimuli using the category-selective localizer. Four regressors indicating the onset of stimuli (duration = 5.45 s) for the 4 image categories were defined. Again, motion parameters, their derivatives, and the cerebrospinal fluid and white-matter signals were modelled as nuisance covariates, and each regressor was convolved with the canonical hemodynamic response function. First-level analysis compared main effects of face- versus scene-related regressors (i.e. house and corridor images where merged together) and vice-versa, which were then used for second level analysis with a one-sample ANOVA. We applied a statistical threshold of $p < 0.05$, corrected for multiple comparisons using family-wise error (FWE) correction at the peak level. This allowed us to delineate two bilateral group-based regions in the fusiform and occipital cortex with greater responses in face vs scene blocks, corresponding to the fusiform face area (FFA, orange cluster in Fig. 3, upper-left insert). Conversely, two regions in the parahippocampal gyrus bilaterally showed greater responses to scene vs face blocks, consistent with the parahippocampal place area (PPA, cyan cluster in Fig. 3, upper-left insert) (Haxby et al., 2001; Kanwisher et al., 1997). Spheres were then drawn at the activation peak (6 mm radius spheres) of the FFA and PPA clusters (left and right) to create functional VOIs and examine category-selective responses to Targets and Salient Distractor during the attentional task.

VOIs analysis. For the attentional task, we first assessed the Target effect on early visual areas (i.e. position VOIs) by creating regressors in our GLM representing the position of the Target stimuli, one for each of the four possible locations, separately for the four task conditions (i.e., cued or uncued trials, with or without the salient face distractor). Because the cueing period and the search period were temporarily close, we defined a combined BOLD response modeled from the onset of the cueing display until the offset of the visual search display (total duration of 2.75 s to cover the entire trial). Estimated motion parameters, their derivatives, plus the cerebrospinal fluid and white matter signals were also included in the GLM as nuisance covariates. All regressors were modeled using the canonical hemodynamic response function. The main effects of conditions were calculated for each event type (i.e., contrasts versus an implicit baseline that covers whatever is not included in the model and reflects overall BOLD signal around events of interest), and the estimated response amplitudes (i.e. beta values) were then extracted within each of the visual VOIs (derived from the position localizer task) when the Target was presented either at this location or elsewhere among the three other possible locations in the display.

Second, we examined responses to the Salient Distractor (i.e. faces) and Target stimuli (i.e. indoor or outdoor scenes) in category-selective areas during the attentional task, using a distinct model with separate regressors for each task contingencies. As above, motion parameters, their derivatives, and the cerebrospinal fluid and white-matter signals were included as nuisance covariate, and each regressor was modeled with a canonical hemodynamic response function. Baseline contrasts were then calculated for each stimulus condition and estimated BOLD amplitudes were extracted within the face- and scene-responsive VOIs for conditions with and without a Salient Distractor presented with the target stimulus, separately for the cued and uncued conditions.

Finally, we extracted estimated BOLD amplitudes within the left and right pulvinar nuclei for each baseline contrasts described above. The left and right pulvinar VOIs were defined from a digital model representing the three-dimensional anatomy of the thalamus and subthalamic structures (Krauth et al., 2010). This pulvinar mask was slightly eroded to limit the impact of adjacent nuclei or white matter and included 20% of the original mask volume. Comparing its extent with previously reported anatomical subdivisions within the pulvinar (Guedj and Vuilleumier, 2020) showed no preferential overlap with any specific subcluster.

The target effect in each position VOIs, and the distractor effect in position VOIs, face/scene VOIs, and pulvinar VOIs, were then considered together in LMM using the same procedure as for behavioral analysis (see Supplementary material, Table S1 for details about random effects selection). We assessed the effect of Cue and Salient Distractor as fixed factors. We added the factor 'VOIs' as a third fixed effect for the position VOIs and face/scene VOIs analyses, and the factor 'Hemisphere' for the pulvinar analysis. Finally, to assess the target effect on position VOIs, the fixed factor 'Presence' (i.e. target appearing at this location vs elsewhere) was also added (see Supplementary material, Table S2 for summary). Because we assumed interactions between fixed factors (at least for Cue and Salient Distractor), we used type III Sums of Squares statistics (Landsheer and van den Wittenboer, 2015; Stewart-Oaten, 1995).

2.6.2. Effect of task contingencies on functional connectivity of pulvinar and attentional networks

Definition of nodes of interest. The importance of frontal-parietal cortical regions in the control of attention is well established, with complementary roles for the ventral and dorsal attention networks (e.g. Corbetta et al. 2008). We therefore selected nodes of interest in these networks following He and colleagues (2007), based on a meta-analysis of four previously published event-related fMRI studies (Astafiev et al., 2004, 2003; Corbetta et al., 2000; Kincade et al., 2005). Four nodes were chosen for the DAN, and two for the VAN. These attentional nodes were used to assess connectivity with the pulvinar and with the visually-responsive nodes delineated by position and face/scene VOIs above (see Supplementary material, Table S2). For this analysis, among the four VOIs identified in early visual cortex, we retained only the two upper occipital areas responding to the lower quadrant because they showed higher selectivity to the target's position. Each node size was defined as a 6 mm radius sphere to match the right and left pulvinar nuclei (i.e. around 50 voxels).

Beta series correlation in the attentional task. To assess the modulation of functional connectivity between attentional networks, pulvinar, and visual areas across the different task contingencies, we used beta series correlation (BSC) analysis (Rissman et al., 2004). This is a method of choice to address functional connectivity in an event-related fMRI design with a priori assumption about predefined regions of interest (Di and Biswal, 2019). Briefly, the BSC method computes correlations of trial-by-trial variability of brain activation across areas. As opposed to standard analyses modeling different task conditions, BSC aims to model patterns of activity on each trial to obtain one beta map per trial. Given the fast event-related task design and the short sampling time of fMRI, we opted for a single-trial-versus-other-trials modelling method (Di and Biswal, 2019; Mumford, 2012). Here, we considered each event (cue onset and search display onset) rather than each trial. To do so, we first built a Generalized Linear Model (GLM) for each event containing two regressors: one for the trial of interest plus a second for all other trials simultaneously. Thus, the GLM design for the first event provides an activation estimate for event 1 and includes a regressor modeling this event and a second regressor modeling all other events. The estimate of $\beta 1$ from this first design corresponds to the single-trial activation for event 1. This process is repeated N times to obtain estimates βs for all N events. The six estimated motion parameters, their derivatives, plus the cerebrospinal fluid and white-matter signals were included in all models as nuisance regressors. Each event had a duration set to 0 and was convolved with a canonical hemodynamic response function. After estimating the beta maps for all successive trials, the average beta values were extracted for each node of interest to derive a beta series for each subject. The beta series were then grouped into four sets representing the four experimental contingencies (i.e. trials with or without a salient face distractor, with or without a spatial cued).

To investigate the effect of task contingencies on functional relationships among nodes, we used the "FSLNets" package from FMRIB Software Library's (FSL, http://fsl.fmrib.ox.ac.uk/fsl/fslwiki/FSLNets) implemented in Matlab. The first step consisted of creating matrices of correlations (Pearson's correlation coefficients) on beta series to estimate, for each subject and task condition, the connection strengths between all nodes. Resulting Fisher's r correlation coefficients were Z-transformed and their average across subjects is presented for each task condition in the Supplementary Material (Fig. S1). Finally, to test for the effect of task contingencies on node interactions, we applied a GLM with inference using the FSL's "Randomise" analysis, a non-parametric permutation test (5000 permutations in each subject) to compare the distribution of values obtained when the condition labels are permuted. We first evaluated the main effects of the Cue and the Salient Distractor, as well as their interaction; and then in a second step evaluated the specific effect of the Salient Distractor in each cue condition. Results were corrected for false-positive errors using $p < 1/N = 0.0055$, where N was the number of possible comparisons (i.e. 14 nodes * 13 nodes). Such correction is a good compromise to control Type I errors without being too strict and likely to increase Type II errors. (i.e., false negatives, e.g. (Bassett and Lynall, 2013; Rothman, 1990).

2.6.3. Dynamic causal modeling (DCM) of pulvinar interactions during the attentional task

Because the BSC analysis does not provide information about directional influences between regions, we applied dynamic causal modeling (DCM) to further estimate the flow of functional interactions among regions within the visual and attentional networks. Briefly, the DCM method draws inferences about neural activity underlying the measured

fMRI data by creating an explicit forward model of how the fMRI signals were caused, based on the hidden neuronal and biophysical state and the resulting hemodynamic modulation. Neural and hemodynamic states are specified by nonlinear differential equations in continuous time with parameters that encode the strength and direction of connections between areas, together with their modulation by experimental factors. These parameters are estimated using the Bayesian statistical framework, so that the predicted fMRI signal of the model fits the observed fMRI data. Causality in DCM implies that the dynamics of one region causes the dynamics of another region in the sense of control theory (Friston, 2009). Different models incorporating different assumptions on the connectivity architecture are constructed in the first step, while the subsequent step of statistical analyses are performed on parameters from the model with the best fit in order to compare the strength of connections across different conditions.

Here, we defined our model space according to a priori hypotheses on attentional and visual networks (see above), further refined by results from the BSC analyses. Hence, full DCM models were estimated including the pulvinar, FFA and its counterpart PPA, as well as pIPS and TPJ, two core nodes of the DAN and VAN networks, respectively. In agreement with the BSC results that revealed effects in both hemispheres (see results below), all selected nodes were defined bilaterally (i.e. merging the right and left seeds), excepted for the TPJ node taken only from the right hemisphere because of the well-known asymmetry of the VAN (Corbetta and Shulman, 2002). To do so, a new set of single-subject GLMs was constructed where the three runs of the main attentional task were concatenated, and three regressors of interest were modelled corresponding to task conditions 'Cue alone', 'Salient Distractor alone' and 'Cue + Salient Distractor'. The implicit baseline corresponded to the uncued condition without salient distractor. This set of GLMs also contained the same regressors-of-no-interest as the previous GLMs. For each node, the first eigenvariate of the BOLD time series was extracted for the DCM analysis and adjusted for effects-of-interest.

We subsequently performed a two-level analysis using Parametric Empirical Bayes (PEB) and Bayesian model comparison (BMC) (Zeidman et al., 2019b). At the first level, a "full model" was specified and estimated for each participant. In this model, the five nodes were bidirectionally connected with each other, and within (intrinsic) connections were also considered (A-matrix). A driving input (C-matrix) was applied to each node, corresponding to the three condition regressors. Cues and/or Salient Distractors (i.e. the three regressors) could serve as driving inputs to every region as we did not include the visual cortex as an "entry" signal in the network. Driving inputs time-series being non-centered, the resulting A-matrix parameters reflect the mean connection weights for the implicit baseline condition (Zeidman et al., 2019a). Finally, based on both BSC results and current knowledge on attentional systems (Vossel et al., 2012), we designed several models (see below) in which the between-region (extrinsic) connection engaging the Pulvinar node or the pIPS node could receive modulatory inputs from either the Cue, the Salient Distractor, or both (B-matrix). At the second level, the DCM parameters of individual participants were fed into a PEB model that decomposes interindividual variability in connection strengths into group effects and random effects.

To test our hypotheses about the role of the connectivity between the pulvinar and the rest of the network, we constructed 12 models, successively pruning away some B-parameters and compared them using BMC. The models were partitioned in two families (i.e. 4×3 models) (Penny et al., 2010) (Fig. 6A). In family F1, the models differed according to which experimental conditions modulated the extrinsic connections: (1) all regressors, (2) Cue alone, (3) Salient Distractor alone, and (4) Cue + Salient Distractor. In family F2, models differed according to the directionality of extrinsic connection influences, including: (1) an influence from the pulvinar to each node of the network, (2) an influence from the pIPS to each node of the network including the pulvinar, (3) a combined influence of the pulvinar and pIPS towards other cortical nodes, with a bidirectional interaction between the pulvinar and pIPS. The selection procedure takes into account the complexity of the models (i.e. the number of B-parameters that allow to modify the connectivity according to the experimental conditions), penalizing the more complex models and selecting the best compromise between accuracy and complexity.

Finally, we used the Bayesian model average (BMA) and averaged parameter values across all models using the posterior model probabilities as weights (Pp). The BMA was thresholded to only retain parameters with a Pp > 95% of being non-zero. We calculated the resulting connectivity value (in Hz) for each modulator input (Zeidman et al., 2019a). Although our main hypotheses concerned changes in effective connectivity due to cues and salient distractors (B-matrix), we also computed the average effective connectivity for the implicit baseline (A-matrix). To obtain these parameters to the group level, we specified and estimated a separate PEB model for the average connectivity A, and performed an automatic search over reduced models using Bayesian model reduction (BMR).

3. Results

3.1. Effect of task contingencies on RTs

Our search task allowed assessing behavioral and neural response patterns according to both task-relevant goals (spatial cueing) and task-irrelevant saliency (face distractor). Accuracy and RT performance during the task, averaged across fMRI runs were summarized in the Table 1. Accuracy was significantly affected by task conditions as shown by the interaction between the Cue and the Salient Distractor ($F(1,29)=27.08$, $p < .0001$). Post-hoc tests revealed a significant decrease in the percentage of correct response in the presence of the Salient Distractor in the uncued condition while it had no effect in the cued condition ($t(29)=5.91$, $p < .0001$). There was no main effect of Cue ($F(1,29)=2.25$, $p > .1$) but a main Distractor effect ($F(1,29)=4.84$, $p < .05$). Beside, RT showed significantly faster target categorization (outdoor/indoor decision) in the presence of the Cue (β = -35.38, SE = 9.70, $\chi^2(1)=13.30$, $p < .001$), whereas the Salient Distractor had no effect (β = -4.19, SE = 9.59, $\chi^2(1)=0.19$, $p = .66$). There was no interaction between Cue and Salient Distractor (β = -0.94, SE = 13.95, $\chi^2(1)=0.005$, $p = .95$). These data show that participants were disturbed by the Salient Distractor presence and efficiently used the cue information, as instructed, while they could successfully ignore the Salient Distractor and achieve similar performance overall.

3.2. Target and salient distractor effects in early and category-selective visual areas

First, we evaluated responses to the Target stimulus across all four visual occipital VOIs (Fig. 2 where betas values were averaged across VOIs). A statistical LMM revealed significantly greater fMRI activation with Presence of the target at the VOI-selective locations compared to other locations in the search display (β=0.74, SE=0.06, $\chi^2(1)=131.59$, $p < .0001$), indicating enhanced processing in retinotopic visual cortex for the task-relevant stimulus. In addition, the concomitant presence of a Salient Distractor significantly impacted target encoding (β=-0.22, SE=0.05 $\chi^2(1)=23.22$, $p < .0001$), consistent with attentional capture and competition for processing resources (e.g. Desimone and Duncan, 1995). Please note this distractor effect at the neural level arose despite the lack of significant impact on RTs at the behavioral level. There was no main effect of Cue (β=0.008, SE=0.05, $\chi^2(1)=0.03$, $p = .86$) or VOIs (average βs=0.04, average SEs=0.67, $\chi^2(3)=6.05$, $p = .11$). We also found interactions between factors, including a quadruple interaction of 'Presence x Cue x Salient Distractor x VOI' (see Table S3-a). Subsequent post-hoc tests on relevant interactions between Presence of the target, Cue, and Salient Distractor showed that when the target location was previously cued, the Salient Distractor did not

Table 1
Behavioral performance.

	Task conditions No Cue No Salient Distractor	No Cue Salient Distractor	Cue No Salient Distractor	Cue Salient Distractor
Accuracy *(% correct trials)*	89 (0.6)	86 (0.5)	88 (0.6)	89 (0.7)
Reaction time *(ms)*	979 (29)	964 (28)	936 (29)	937 (30)

Data represent mean (± standard error)

affect neural activity in the VOI coding for this location (t(115299)=-1.66, p = .1), whereas the response to Target decreased when competing with a Salient Distractor in the absence of the Cue (t(115299)=3.5, p = .0005). This is consistent with a "protective" effect of the cue against the impact of Salient Distractors.

Second, we assessed the task contingency effects on the category-selective areas FFA and PPA (Fig. 3). The Salient Distractor significantly modulated both visual areas (β = -0.29, SE = 0.03, χ^2(1)=76.17, p < .0001), whereas the Cue and VOIs showed no main effect. More crucially, post-hoc tests revealed significant interactions (see Table S3-b) indicating that the Salient Distractor (face) increased activity in FFA but decreased activity in PPA (β=0.59, SE=0.05, χ^2(1)= 154.13, p < .0001). This is consistent with a competition between the representation of scene targets and face distractors. In addition, a triple interaction (β=0.23, SE=0.07, χ^2(1)= 11.38, p = .001) showed that the Cue also affected the FFA activity by increasing its response mainly on trials with a Salient Distractor relative to trials without a Salient Distractor (t(29921)=-4.49 and t(29921)=-11.99, all ps<.0001), while there was no such modulation for PPA (t(29921)=-0.74 and t(29921)=-1.53, all ps>.1) regardless of Salient Distractor. This finding suggests an influence of the Cue on the bottom-up processing of the Salient Distractor, again without overt effects at the behavioral level.

3.3. Pulvinar activity is sensitive to both salient and relevant stimuli

We next examined pulvinar activity during the attentional task as a function of the Cue and Salient Distractor stimuli, across the two hemispheres (left or right). Results (Fig. 4, see also Table S3-c) showed a significant main effect of Salient Distractor (β=-0.07, SE=0.02, χ^2(1)=10.49, p = .001), together with an interaction with Cue (β=0.2, SE=0.02, χ^2(1)=15.29, p < .0001) and hemisphere (β=0.08, SE=0.03, χ^2(1)=6.75, p < .01), as well as a triple interaction (β=-0.13, SE=0.05, χ^2(1)=7.92, p < .01). Post-hoc tests revealed that this reflected a significant increase in left pulvinar activity on cued trials and decrease on uncued trials in the presence of Salient Distractor (t(12090)=-2.29, p < 0.02 and t(12090)=3.24, p < 0.001), while left pulvinar activity was unaffected by the cue in the absence of the Salient Distractor (t(12090)= 0.90, p = .37). These effects were not significant in the right pulvinar. Note that this effect was also visible on standard whole-brain analysis, but at an uncorrected threshold for multiple comparisons (see Supplementary Material, Fig. S2). Indeed, the detection of activation in the thalamus is known to be challenging due to the small size of subcortical nuclei associated with large inter-individual variability (Llano, 2013).

Taken together, these results suggest that the pulvinar (on left side in particular) is differentially reactive to salient information such as the onset of a task-irrelevant face, but this response is dependent on current top-down signals associated with the Cue and hence the potential conflict with task-relevant inputs.

3.4. Modulation of task-induced functional connectivity of the pulvinar

We next turned to our main question concerning functional interactions of the pulvinar with other brain areas during selective attention. First, we used the BSC method to estimate trial-by-trial activity and reciprocal correlation between nodes of our pre-defined network of visual and attentional areas. These time-series reflect changes in the functional recruitment and coupling of these regions according to task demands. The correlation matrices computed for each task condition separately indicated that the connectivity within this network was always positive (see Supplementary Material, Fig. S1) but significantly modulated across conditions. We then assessed the respective effect of Cue and Salient Distractor, as well as their interaction, on these functional connectivity patterns within the attention and visual networks (Fig. 5A).

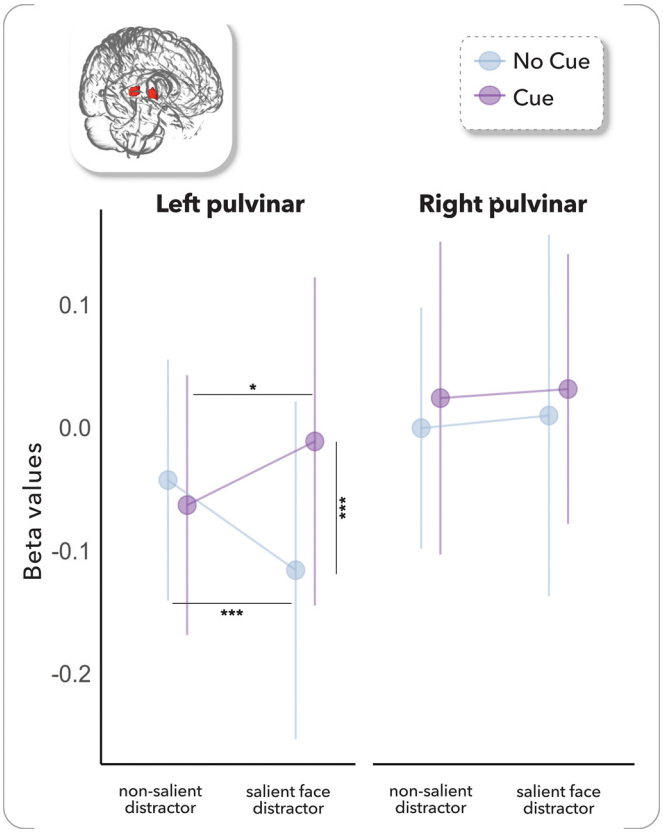

Fig. 4. Cue and Salient distractor effects on pulvinar activity. Anatomically defined left and right pulvinar nuclei (red cluster) are depicted on a 3D rendering brain view [top-left insert]. Mean beta values are shown for each nucleus according to the different task contingencies. Error bars reflect the standard errors of the mean. (Relevant post-hoc tests: ***p-value < 0.001; **p-value < 0.01; *p-value < 0.05).

Results showed a significant main effect of the Cue, which reduced connectivity strength (compared to No Cue condition) between the left PPA and right TPJ (average z-score difference = -0.08), as well as between the right PPA and V1-V2 nodes (coding for the bottom-right quadrant) (average z-score difference = -0.07), and between the right FFA and the same V1-V2 areas (average z-score difference = -0.07, all ps<.004) (see also Fig. 5B). There was no main effect of Distractor but

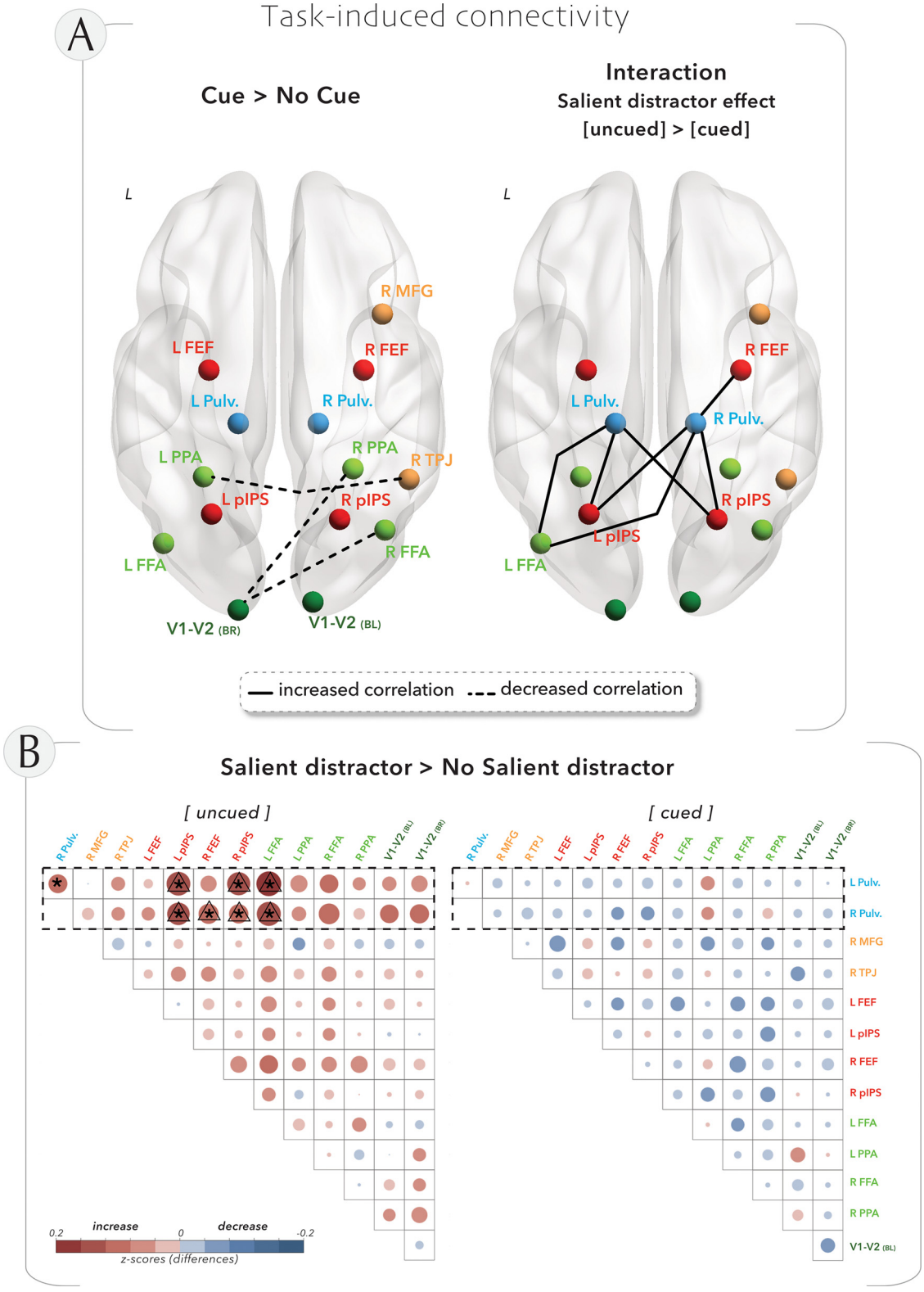

Fig. 5. Task-induced connectivity estimated by beta series correlation (BSC) analysis in the attentional task. We defined an a priori network of interest comprising nodes in the ventral (orange dots) and dorsal (red dots) attention networks, nodes in early (dark green dots) and late (light green dots) visual areas, as well as the left and right pulvinar nuclei (blue dots) as anatomically defined. (A) We evaluated the effect of Cue [left panel], (and see also the corresponding matrix in B), Salient Distractor (no significant effect, not shown), and their interaction [right panel] on functional connectivity. Significant increases in connectivity are represented by solid lines, and significant decreases by dashed lines. (B) Matrix of functional connectivity differences between Cue vs. No Cue conditions (C) Matrices of functional connectivity differences between conditions with vs. without a Salient Distractor, showed separately for the uncued [left panel] and cued [right panel] conditions to illustrate the significant interaction between these factors. Significant changes in the matrices are indicated with asterisks. Those found in the interaction contrast are also marked with a triangle. Abbreviations: R= right hemisphere; L = left hemisphere; FFA: fusiform face area; FEF: frontal-eye-field; MFG: middle frontal gyrus; pIPS: posterior intraparietal sulcus; PPA: parahippocampal place area; Pulv.: pulvinar; TPJ: temporo-parietal junction.

a significant interaction between the Cue and the Salient Distractor that selectively modulated connections of both left and right pulvinar.

Specifically, in response to the Salient Distractor on uncued trials (as compared to cued trials), the left pulvinar showed significantly higher coupling strength with left FFA and pIPS (average z-score difference = -0.18 for both connections, ps<.002), as well as with contralateral (right) pIPS (average z-score difference = -0.17, ps<.001) and contralateral (right) FFA to a lesser (non-significant) degree (difference = -0.12). Similarly, in the same condition, the right pulvinar also showed higher coupling strength with right pIPS and FEF (average z-score difference = -0.14 for both connections, ps<.006), and with contralateral (left) pIPS and FFA (average z-score difference = -0.15 and -0.18 respectively, ps<.005). In addition, dissecting these effects separately for each cueing condition, we found that the Salient Distractor (Fig. 5C) also produced a significant increase of inter-hemispheric functional connectivity between the two pulvinar nodes in the uncued condition, while it had no such effect in the cued condition. These modulations of pulvinar connectivity may echo the pattern of pulvinar activity described above where the Salient Distractor produced distinct effects depending on the cue condition, and further suggest a shielding or "protective" influence of the cue on responses to the Salient Distractor. Moreover, remarkably, the changes in trial-by-trial functional connectivity observed here affected both pulvinar nodes in symmetric ways, despite the fact we found no significant modulation of overall activity magnitude for the right pulvinar in VOI analysis (see above).

Altogether, these results confirm that the pulvinar and its functional connectivity are particularly sensitive to interactive influences between the cue effects and the distractor effects. In addition, they point to a direct interplay of this region with bilateral pIPS and right FEF, two core regions of the dorsal attentional network controlling top-down attention, as well as with FFA encoding bottom-up visual information from the salient face distractor.

3.5. Causal functional interactions of pulvinar with visual and attentional areas

Finally, we used DCM to probe how each task condition modulated directional influences between the pulvinar and the rest of our predefined network. To this aim, we designed DCMs connecting the pulvinar to all other nodes of the network, without assuming direct connections between the latter except for a connection between pIPS and TPJ previously postulated in a standard model of attention (Corbetta et al., 2008). Based on results from our BSC analysis, we compared 12 connectivity models divided into two families (see Fig. 6A), respectively defined according to which experimental condition had a modulatory effect (family 1), and which direction mediated the effect (family 2).

The BMC statistics performed on these DCMs clearly selected a final model merging the attributes of model 4 from the first family with parameters of model 3 from the second family as the most plausible architecture (Fig. 6A, winning models highlighted by a blue inset; Pp > 84%), indicating that all experimental conditions had a modulatory effect on connections from the pulvinar to cortical regions within the network. Interestingly, we note the model ranking second (with Pp = 15%) implied attributes from model 3 in the first family which assumed a modulation of pulvinar connections only for the condition 'Cue + Salient Distractor'. These data converge with other results above to suggest that the pulvino-cortical dialogue is particularly influenced by attentional signals integrating both endogenous cues and stimulus salience effects, rather than just one or the other.

To identify the changes in effective connectivity evoked by the cues and salient distractors, we first estimated the average functional connectivity for the implicit baseline condition (i.e. A-matrix parameters), corresponding to trials without a spatial cue and without a face distractor. To do so, we performed BMR on a 'full' model with all possible connections between nodes. The results are shown in Fig. 6B (all Pp > 95%). In the absence of endogenous or exogenous signals (baseline), all regions exhibited self-inhibition. Within this network, all extrinsic connections had a positive influence excepted for FFA to pIPS (-0.08 Hz) and pIPS to TPJ (-0.07 Hz). Thus, the pulvinar sent excitatory inputs to TPJ (0.10 Hz), pIPS (0.09 Hz), and PPA (0.07 Hz), while it received a reciprocal excitatory input from PPA (0.13 Hz). The highest extrinsic connectivity was between PPA and FFA (0.23 Hz), possibly reflecting competition between the target 'scene' and the distractor 'face' stimuli (see Fig. 3).

Next and most critically, we determined significant modulatory effects (i.e. B-matrix parameters) in the 'winning' model selected from the BMC. As shown in Fig. 6B, different connections were modulated by different experimental conditions. The presence of the cue strongly and selectively increased the positive connectivity from pulvinar to pIPS (0.71 Hz), presumably involved in goal-directed top-down attention. On the other hand, the presence of a Salient Distractor increased the positive connectivity from pulvinar to FFA (0.27 Hz), an effect that was strongly amplified by a concomitant occurrence of the Cue (0.52 Hz). In contrast, the pulvinar input to pIPS was lower in the presence of both the Salient Distractor and the Cue relative to the Cue only (0.23 vs 0.71 Hz), but still higher than in the baseline condition (0.15 Hz). Moreover, in the condition with the Cue and Distractor presented together, the pulvinar sent excitatory connections to all nodes of the network. The strongest inputs were toward FFA and TPJ, two nodes potentially involved in bottom-up attentional capture by the distractor face. These excitatory inputs from pulvinar as well as those to PPA were also stronger in this condition than in baseline (see Fig. 6). Altogether, these data support a central role of the pulvinar in integrating different sources of attentional signals, e.g., when confronted with both exogenous and endogenous influences, which produced a significant enhancement of its projections toward several cortical areas in the visual and attentional systems.

4. Discussion

We tested the respective and joint influence of goal-relevant endogenous cues and task-irrelevant salient distractors in a visual attention task where participants were asked to judge a target presented among non-target stimuli. Specifically, our analysis focused on the modulation of the pulvinar functional connectivity with occipito-temporal and frontoparietal areas involved in selective attention. Firstly, we characterized the impact of target and distractor stimuli on visual areas in order to evaluate stimulus processing in cortical pathways, as well as their effects on pulvinar activity across different task conditions. Secondly, we measured functional connectivity within a network comprising visual areas and a priori selected regions in the VAN and DAN to assess their dynamics with the pulvinar under the different task conditions. To do so, we designed a visual task that orthogonally manipulated top-down selection (with or without a predictive spatial cue) and bottom-up competition (with or without a task-irrelevant distractor) while participants had to orient attention to a visually defined singleton target. Our results show that pulvinar activity and connectivity exhibited a distinctive pattern of engagement according to the co-occurrence of both the cue and the distractor, rather than being driven by one of these factors presented alone. These data point to a key role of the pulvinar in integrating different (and potentially conflicting) sources of attentional guidance.

4.1. Interaction of top-down attention control and bottom-up pre-attentive salience in visual areas

When a spatially uninformative cue was presented, participants had to distribute their attention over the entire search screen in order to report the target, such that the appearance of a salient face distractor amidst the display required inhibiting its representation and suppressing any response to it. In contrast, the informative cue (100% valid) allowed participants to focus their endogenous attention to the target location and hence optimize their processing resources toward the task-relevant

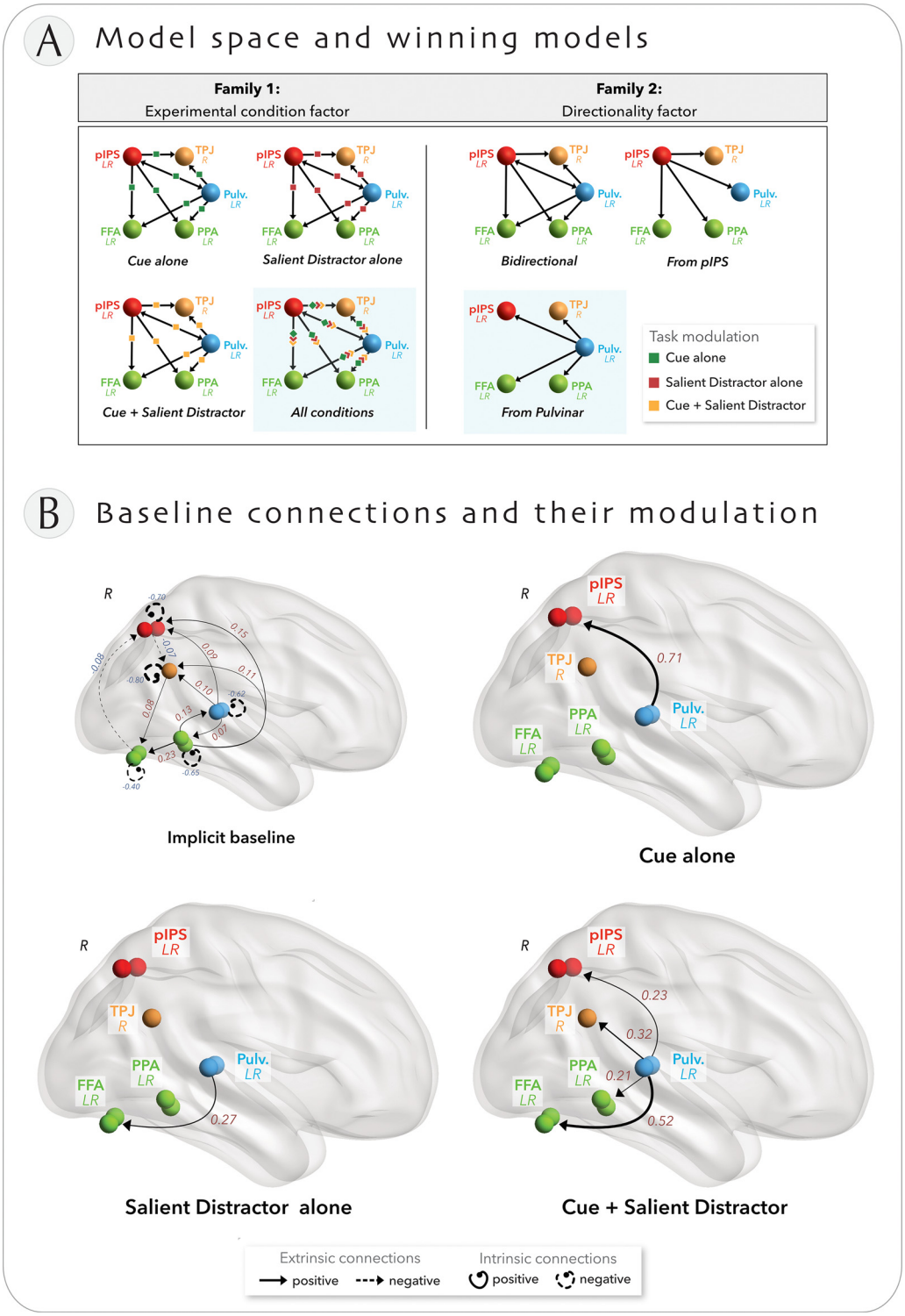

Fig. 6. Dynamic causal modeling. (A) Model space for the DCM analysis including 5 nodes (pulvinar, PPA, FFA, TPJ and pIPS merged from both hemispheres, excepted for TPJ that is only right-sided to accord with previous literature) and 3 experimental task conditions (Cue alone, Salient Distractor alone, Cue + Salient Distractor). The full model included driving inputs to each node from all experimental conditions, intrinsic connections for each node, bidirectional extrinsic connections between nodes, and modulations of Pulvinar and pIPS connections by experimental conditions (green, red, and yellow arrows with square tip, respectively). We constructed 12 models partitioned in two families: family 1 comparing which experimental conditions modulated the extrinsic connections, and family 2 comparing which directionality of the extrinsic connections predominated. Winnings models in each family are highlighted in blue. (B) Influence of task conditions on effective connectivity. All represented connections had a posterior probability (Pp) of at least 0.95. The dark red and dark blue numbers indicate respectively the excitatory and inhibitory strength of directed coupling (quantified in Hz). Note that by default, intrinsic connection have no units but are scaled up or down from the default self-connection of 0.5 Hz. The width of the arrows is proportional to the strength of coupling. Connectivity during the implicit baseline, i.e. in the absence of cues and salient distractors (A-matrix parameters) [top-left brain diagram]. Modulation effects of the wining model by the experimental condition (B-matrix parameters): (1) the effect of Cue alone [top-right brain diagram], (2) the effect of Salient Distractor alone [bottom-left brain diagram], and (3) the effect of Cue + Salient Distractor presented together [bottom-right brain diagram]. Abbreviations: L = left hemisphere; FFA: fusiform face area; pIPS: posterior intraparietal sulcus; Pulv.: pulvinar.

stimulus (Petersen and Posner, 2012; Reynaud et al., 2019; Reynolds et al., 1999).

Despite the simplicity of the task, primarily designed for fMRI rather than precise psychophysical testing, we found a significant modulation of behavioral performance by task conditions. As expected, accuracy was significantly impact by the Salient Distractor presence in uncued trials, and reaction times showed that target detection was faster with a valid than an uninformative cue, indicating that participants did use and benefited from spatial cueing. In contrast, the presence of a salient face distractor did not produce a significant behavioral effect on RTs, but it had a clear impact at the neural level. Not only the task-irrelevant face increased the response of FFA, but it also decreased the response evoked by the target in early retinotopic visual cortex (particularly in the no-cue condition) as well as the PPA (regardless of cue condition). These data, taken with accuracy scores, clearly suggest a cost for the target scene representation due to competition with the salient face distractor.

Theoretically, attentional capture by a salient distractor can be inhibited at several levels of the processing hierarchy and its impact on search depends on its access to a "priority" map governing the current focus of attention (Wolfe, 2021). Here, consistent with the fact that endogenous spatial control acts on the pre-attentive processing of salience signals (Geyer et al., 2010), our results revealed an interaction between the Cue and Salient Distractor for both early visual cortex and FFA – although with a different pattern. With a non-informative cue, the salient distractor led to decreased activity in functionally defined occipital VOIs coding for the position of the target or other positions in the search display, while these visual areas showed no cost of the distractor when attention was oriented to the target's position by the Cue. This pattern demonstrates a clear "shielding" effect of spatial cueing against distraction induced by salient but task-irrelevant information.

In parallel, top-down spatial selection was counterbalanced by the intrinsic saliency of face stimuli (End and Gamer, 2017; Hernández-García et al., 2020), presumably competing in priority map with the colored target singleton at a later stage of visual processing. Remarkably, in the presence of the cue, the face distractor evoked higher activity in the category-selective FFA VOI, rather than lower activity as would be predicted by a direct suppression of visual inputs from task-irrelevant positions in the display. Although counterintuitive at the first sight, FFA increased activity fully accords with the perceptual load account of attentional selection (Lavie et al., 2003), whereby the cue could reduce visual demands for target identification (i.e., perceptual load) and thus increase residual processing resources to process distracting and task-irrelevant stimuli in the display.

Taken together, our findings converge with goal-driven theories (Eimer and Kiss, 2010; Folk et al., 1992; Gaspelin and Luck, 2018) by showing that endogenous attention control can act to select relevant information according to current task demands and prevent overt orienting to the location of irrelevant distractors, even though distractor information can still be processed pre-attentively. Accordingly, it has been shown that salient stimuli may summon attention but be inhibited by an active suppressive mechanism before attentional shifting occurs in order to avoid overt interference (Gaspelin and Luck, 2019, 2018), and goal-driven spatially directed selection may play a key role in this inhibitory process (Feldmann-Wüstefeld et al., 2021). More generally our data indicate that multiple sources of influences need to be integrated in the "priority map" guiding selective attention, a computation that is likely to involve broader networks including fronto-parietal areas and pulvinar (Bourgeois et al., 2020; Guedj and Vuilleumier, 2020).

4.2. Activation patterns in the pulvinar follow sensory responses in different visual areas

At the pulvinar level, we again found a significant interaction between the Cue and Salient Distractor. Specifically, in the left pulvinar, activity was reduced when the face distractor was present and the cue was absent, similar to early visual areas; while conversely it was increased when both the face distractor and the cue were presented together, similar to the FFA. In other words, spatial cueing to the relevant target location recruited the pulvinar only during competition with another salient, task-irrelevant stimulus. However, no significant modulation was observed in the right pulvinar (see also Hakamata et al., 2016 and Padmala et al., 2010 for similar left-sided pulvinar asymmetries). It is unclear whether this asymmetry reflected a temporal component mediated by the left hemisphere (Coull and Nobre, 2008) given the preparatory delay between the cue and the search display, the use of the right hand to report targets, or other factors. Moreover, connectivity results were generally symmetrical for both sides.

In any case, this interaction pattern in (left) pulvinar points to a specific role in integrating sensory inputs from different visual areas with concomitant top-down signals, e.g., through either inhibitory or amplificatory projections. Previous research in the monkey reported that exciting lateral pulvinar neurons can boost the visual response of V1 neurons with the same receptive field and suppress responses to the surrounding visual field (Purushothaman et al., 2012). A similar pulvinar-mediated mechanisms might operate in our task to enable the Cue to counteract the suppressive effect of the Salient Distractor on activity of early visual areas, possibly acting to increase the attentional weight of target position in the priority map (Fang et al., 2020). A modulatory role of the pulvinar has also been shown in higher-order visual areas (de Souza et al., 2020). For example, silencing pulvinar neurons in the cat was found to alter the contrast response function of cortical neurons in both areas 17 and 21a (homologs of V1 and V4, respectively), with the largest effect observed in the latter.

The similarity of modulations observed in the left pulvinar with those of both FFA and early occipital areas, supports the hypothesis that transthalamic visual pathways are functionally specific to their cortical target (Blot et al., 2021). They differ from feedforward cortical pathways by combining information from multiple brain regions, linking sensory signals to the behavioral context. This notion also agrees with previous studies reporting a variety of signals in pulvinar neurons related to both the focus of attention and task goals (Halassa and Acsády, 2016; Komura et al., 2013; Saalmann et al., 2012; Zhou et al., 2016). However, the extent to which the pulvinar can directly regulate activity of higher-order visual areas remains to be determined (de Souza et al., 2020; Soares et al., 2004; Zhou et al., 2016), and further studies inducing transient inactivation of specific pulvino-cortical loops will be crucial to resolve this issue. In any case, these data converge to support an integrative role of the pulvinar (Guedj and Vuilleumier, 2020), as further suggested by our functional connectivity analyses.

4.3. The pulvinar as a conductor of cortical dynamics

In keeping with the above, the main objective of our study was to determine how different priority signals from top-down and bottom-up sources induced by task contingencies engaged the pulvinar and modulated its functional coupling with distant cortical areas within visual and attentional networks.

Our connectivity analyses provided additional evidence in support of a specific role in combining these signals by coordinating activity among multiple cortical areas. Remarkably, neither the main effect of Cue nor the main effect of Salient Distractor had a distinct impact on pulvinar connectivity. A main effect of Cue, directing attention to the target location, was only found to decrease the connectivity between left PPA, presumably related to the target stimulus processing, and right TPJ, a key node of the VAN, as well as the connectivity of both FFA and PPA with early visual cortex. The pulvinar did not show any significant change in connectivity for this contrast. Reduced functional coupling among TPJ and visual areas might reflect a lower recruitment of the VAN when attention was guided by the 100% valid cue (Corbetta et al., 2008), without the need to reallocate attention after orienting to a non-target location.

On the other hand, pulvinar functional connectivity was selectively sensitive to the interaction between the Cue and the Salient Distractor. In particular, the pulvinar exhibited a lower coupling with the pIPS bilaterally, right FEF, and FFA when the Salient Distractor appeared on cued trials, compared to uncued trials. This modulation was observed on both sides, despite the lack of significant change in overall activity seen in right pulvinar (see above). Furthermore, the DCM results revealed that the pulvinar mainly acted through excitatory connections to all cortical areas in the network, but with differential weights depending on task conditions and more widespread influences in trials with both a Cue and a Salient Distractor. These directional influences of pulvinar on other regions comprised an input toward FFA related to the face distractor (even when presented alone) and an input toward pIPS related to the cue (even when presented alone), with the former being strengthened and the latter attenuated when the Cue and Distractor appeared together.

Pulvinar inputs to pIPS might serve to increase the top-down influence weight of parietal cortex on the early visual areas in order to direct the attentional focus to the target location (Fiebelkorn et al., 2019), in line with the well-established role of pIPS in endogenous spatial attention (e.g. Corbetta and Shulman 2002, Gillebert et al. 2011, Martín-Arévalo et al. 2021, Vuilleumier et al. 2008). Competitive interactions between relevant and irrelevant stimuli occur in pIPS neurons, reflecting a convergence of both top-down and bottom-up representations in spatial priority maps that guide attention to task-relevant stimuli (Bisley and Goldberg, 2010; Gottlieb et al., 1998; Ptak, 2012). Unlike parietal areas, the pulvinar contains only coarse retinotopic maps in its ventral part which may not allow for a fine-grained representation of visual space (Arcaro et al., 2015; Shipp, 2003; Silver and Kastner, 2009) but nonetheless interact with visually selective neurons in V1/V2 (de Souza et al., 2020; Purushothaman et al., 2012). Increased coupling of pulvinar with pIPS and FEF on uncued trials, without concomitant increases in driving inputs in DCM, could reflect a greater engagement of top-down processes from attention control systems in DAN in order to focus on the target location and ignore the distractor location in these trials.

Conversely, the causal input from pulvinar to FFA was not only enhanced by the salient distractor, but also stronger in the cued than the uncued condition. This might be consistent with an active inhibitory process acting to suppress the task-irrelevant face stimuli, similar to preattentive signal suppression mechanisms counteracting involuntary attentional capture (Gaspelin and Luck, 2018), more efficient in the presence of the spatial cue (Feldmann-Wüstefeld et al., 2021; Foster et al., 2020). This would in turn accord with the pulvinar having a strategic role in gating sensory information flow in cortical areas (Fiebelkorn et al., 2019; Green et al., 2017; Jaramillo et al., 2019; Saalmann et al., 2012; Zhou et al., 2016) that eventually serves to resolve competition when two salient stimuli (e.g. face distractor and color singleton) generate two “hot spots” within attention priority map.

Hence, although results from our two functional connectivity analysis (BSC and DCM) might appear counterintuitive at first sight, they actually provided highly complementary information. As just noted, functional coupling of the pulvinar was increased with pIPS, FEF and FFA in response to the Salient Distractor in absence of the Cue in BSC results, while its inputs to IPS and FFA were stronger in response to Salient Distractor presented together with the Cue in DCM results. However, both approaches yield different insights on functional interactions between brain areas. Increased connectivity of the pulvinar with visual and attentional networks in BSC should be interpreted as a co-activation of these brain regions, modulated by the task demand, whereas DCM provides an estimate of causal influences of one region on others within a given modeled network (Daunizeau et al., 2011; Friston, 2011). In the context of our task, when search was not guided by a spatially valid cue, efficient goal-directed attention would presumably require both enhancing an active preattentive suppression mechanism to ignore the spatial position of distractors (*Signal Suppression Hypothesis*, Gaspelin and Luck, 2019), together with stronger top-down drive from endogenous control networks to resist to attentional capture and focus on task-relevant stimuli (Corbetta and Shulman, 2002; Kastner and Ungerleider, 2000). We surmise that these two effects might be orchestrated though pulvinar inputs to cortical regions, and account for differential increases of activity and connectivity in FFA and IPS/FEF depending on co-occurrence of the Cue and the Distractor. We note however that interpreting DCM results for fMRI in terms of activation/inhibition remains challenging given the diversity of neuronal populations (i.e., inhibitory and excitatory neurons) present in voxel (Daunizeau et al., 2011). In any case, these complementary insights gained from BSC and DCM analysis further highlight a key function of the pulvinar in fine-tuning neural processes allowing selective information processing and goal-directed behavior, in a context-dependent manner (Saalmann and Kastner, 2011). This coordination function might be implemented either by direct modulatory signals to bias processing in specific areas or by more indirect influences regulating information transfer between cortical (and subcortical) areas (Al-Aidroos et al., 2012; Saalmann et al., 2012), possibly through a synchronization of oscillatory neuronal activity across networks (Bourgeois et al., 2020; Fiebelkorn et al., 2019; Saalmann et al., 2012). Further investigation with electrophysiology techniques will be required to clarify these issues.

5. Conclusion

Altogether, our connectivity results shed new light on the dynamics of pulvinar interactions with other brain areas. However, although our BSC analysis and DCM models were defined with strong a priori based on previous research in order to ensure a good Bayesian estimation power, it should be acknowledged that real brain dynamics is much more complex and further studies are warranted to more precisely characterize the pulvino-cortical interactions. In addition, further research with advanced high-resolution MRI techniques is needed to better dissect any differential role of functional subclusters within the pulvinar (Guedj and Vuilleumier, 2020). Time-resolved techniques with source localization methods would also be valuable to track the precise time-course of reciprocal influences between cortical and subcortical areas during attentional processing.

Nevertheless, our study extends previous work in novel ways. In keeping with the notion that the pulvinar may entertain a unique anatomy by being connected with almost the entire brain (Kaas and Lyon, 2007; Shipp, 2003), we provide new evidence for highly specific pulvino-cortical influences. We conclude these may allow for the flexible orchestration and integration of both top-down and bottom-up signals among distributed networks, essential to shape attentional priority maps across space and modalities.

Data availability statement

All relevant codes and final data (i.e. thresholded maps of the standard GLM, examples of onset and nuisance regressor files used in the BSC analysis, and final DCM outputs) are available here : 10.26037/yareta:tcivcn4swrdrvkv7lb7zloqtpm

Raw data that support the findings of this study are available from the corresponding author, without any restrictions.

Declaration of Competing Interest

None.

Credit authorship contribution statement

Carole Guedj: Conceptualization, Data curation, Formal analysis, Investigation, Methodology, Project administration, Resources, Software, Validation, Visualization, Writing – original draft, Writing – review & editing. **Patrik Vuilleumier:** Conceptualization, Funding acquisition,

Methodology, Project administration, Supervision, Validation, Writing – review & editing.

Data availability

Part of codes and data will be available with a link.

Acknowledgments

This work was supported by two project grants from the Swiss National Science Foundation to PV [grant numbers 320030_166704 and 320030_192792] and a Young Investigator grant from the Novartis Foundation for medical-biological Research to CG. The authors would also like to thank Dr. Peter Zeidman for his guidance in the DCM analysis, and Bruno Bonet and Frédéric Grouiller for their assistance with the data collection and MRI methodology. This study was conducted using the imaging platform at the Brain and Behaviour Laboratory (BBL), University of Geneva.

Supplementary materials

Supplementary material associated with this article can be found, in the online version, at doi:10.1016/j.neuroimage.2022.119832.

References

Al-Aidroos, N., Said, C.P., Turk-Browne, N.B., 2012. Top-down attention switches coupling between low-level and high-level areas of human visual cortex. Proceedings of the National Academy of Sciences 109, 14675–14680. https://doi.org/10.1073/pnas.1202095109.

Astafiev, S.V., Shulman, G.L., Stanley, C.M., Snyder, A.Z., Van Essen, D.C., Corbetta, M., 2003. Functional organization of human intraparietal and frontal cortex for attending, looking, and pointing. J. Neurosci. 23, 4689–4699. doi:10.1523/JNEUROSCI.23-11-04689.2003.

Astafiev, S.V., Stanley, C.M., Shulman, G.L., Corbetta, M., 2004. Extrastriate body area in human occipital cortex responds to the performance of motor actions. Nat. Neurosci. 7, 542–548. doi:10.1038/nn1241.

Bassett, D.S., Lynall, M.E., 2013. Network methods to characterize brain structure and function. In: Gazzaniga, M.S., Ivry, R.B., Mangun, G.R. (Eds.), Cognitive Neurosciences: The Biology of the Mind. MIT Press, Cambridge, MA.

Bates, D., Mächler, M., Bolker, B., Walker, S., 2015. Fitting linear mixed-effects models using lme4. Journal of Statistical Software 67 (1), 1–48. https://doi.org/10.18637/jss.v067.i01.

Bertini, C., Pietrelli, M., Braghittoni, D., Làdavas, E., 2018. Pulvinar lesions disrupt fear-related implicit visual processing in hemianopic patients. Front. Psychol. 9. doi:10.3389/fpsyg.2018.02329.

Bisley, J.W., Goldberg, M.E., 2010. Attention, intention, and priority in the parietal lobe. Annu. Rev. Neurosci. 33, 1–21. doi:10.1146/annurev-neuro-060909-152823.

Bourgeois, A., Guedj, C., Carrera, E., Vuilleumier, P., 2020. Pulvino-cortical interaction: an integrative role in the control of attention. Neurosc. Biobehav. Rev. 111, 104–113. doi:10.1016/j.neubiorev.2020.01.005.

Chalfin, B.P., Cheung, D.T., Muniz, J.A.P.C., de Lima Silveira, L.C., Finlay, B.L., 2007. Scaling of neuron number and volume of the pulvinar complex in new world primates: comparisons with humans, other primates, and mammals. J. Comp. Neurol. 504, 265–274. doi:10.1002/cne.21406.

Corbetta, M., Kincade, J.M., Ollinger, J.M., McAvoy, M.P., Shulman, G.L., 2000. Voluntary orienting is dissociated from target detection in human posterior parietal cortex. Nat. Neurosci. 3, 292–297. doi:10.1038/73009.

Corbetta, M., Patel, G., Shulman, G.L., 2008. The reorienting system of the human brain: from environment to theory of mind. Neuron 58, 306–324. doi:10.1016/j.neuron.2008.04.017.

Corbetta, M., Shulman, G.L., 2002. Control of goal-directed and stimulus-driven attention in the brain. Nat. Rev. Neurosci. 3, 201–215. doi:10.1038/nrn755.

Cortes, N., de Souza, B.O.F., Casanova, C., 2020. Pulvinar modulates synchrony across visual cortical areas. Vision 4, E22. doi:10.3390/vision4020022, (Basel).

Coull, J.T., 1998. Neural correlates of attention and arousal: insights from electrophysiology, functional neuroimaging and psychopharmacology. Prog. Neurobiol. 55, 343–361.

Daunizeau, J., David, O., Stephan, K.E., 2011. Dynamic causal modelling: A critical review of the biophysical and statistical foundations. NeuroImage 58, 312–322. https://doi.org/10.1016/j.neuroimage.2009.11.062.

De Souza, B.O.F., Cortes, N., Casanova, C., 2020. Pulvinar Modulates Contrast Responses in the Visual Cortex as a Function of Cortical Hierarchy. Cereb Cortex 30, 1068–1086. https://doi.org/10.1093/cercor/bhz149.

Desimone, R., Duncan, J., 1995. Neural mechanisms of selective visual attention. Annu. Rev. Neurosci. 18, 193–222. doi:10.1146/annurev.ne.18.030195.001205.

Di, X., Biswal, B.B., 2019. Toward task connectomics: examining whole-brain task modulated connectivity in different task domains. Cereb. Cortex 29, 1572–1583. doi:10.1093/cercor/bhy055.

Eimer, M., Kiss, M., 2010. Top-down search strategies determine attentional capture in visual search: behavioral and electrophysiological evidence. Atten. Percept. Psychophys. 72, 951–962. doi:10.3758/APP.72.4.951.

End, A., Gamer, M., 2017. Preferential processing of social features and their interplay with physical saliency in complex naturalistic scenes. Front. Psychol. 8, 418. doi:10.3389/fpsyg.2017.00418.

Fang, Q., Chou, X., Peng, B., Zhong, W., Zhang, L.I., Tao, H.W., 2020. A differential circuit via retino-colliculo-pulvinar pathway enhances feature selectivity in visual cortex through surround suppression. Neuron 105, 355–369. doi:10.1016/j.neuron.2019.10.027, e6.

Fecteau, J.H., Munoz, D.P., 2006. Salience, relevance, and firing: a priority map for target selection. Trends Cogn. Sci. 10, 382–390. doi:10.1016/j.tics.2006.06.011.

Feldmann-Wüstefeld, T., Weinberger, M., Awh, E., 2021. Spatially Guided Distractor Suppression during Visual Search. J. Neurosci. 41, 3180–3191. https://doi.org/10.1523/JNEUROSCI.2418-20.2021.

Fiebelkorn, I.C., Pinsk, M.A., Kastner, S., 2019. The mediodorsal pulvinar coordinates the macaque fronto-parietal network during rhythmic spatial attention. Nat. Commun. 10. doi:10.1038/s41467-018-08151-4.

Fischer, J., Whitney, D., 2012. Attention gates visual coding in the human pulvinar. Nat. Commun. 3, 1051. doi:10.1038/ncomms2054.

Folk, C.L., Remington, R.W., Johnston, J.C., 1992. Involuntary covert orienting is contingent on attentional control settings. J. Exp. Psychol. Hum. Percept. Perform. 18, 1030–1044.

Friston, K., 2009. Causal modelling and brain connectivity in functional magnetic resonance imaging. PLoS Biol. 7, e1000033. doi:10.1371/journal.pbio.1000033.

Friston, K.J., 2011. Functional and Effective Connectivity: A Review. Brain Connectivity 1, 13–36. https://doi.org/10.1089/brain.2011.0008.

Friston, K.J., Holmes, A.P., Worsley, K.J., Poline, J.P., Frith, C.D., Frackowiak, R.S.J., 1994. Statistical parametric maps in functional imaging: a general linear approach. Hum. Brain Mapp. 2, 189–210. doi:10.1002/hbm.460020402.

Gaspelin, N., Luck, S.J., 2018. The role of inhibition in avoiding distraction by salient stimuli. Trends Cogn. Sci. 22, 79–92. doi:10.1016/j.tics.2017.11.001.

Gaspelin, N., Luck, S.J., 2019. Inhibition as a potential resolution to the attentional capture debate. Curr Opin Psychol 29, 12–18. https://doi.org/10.1016/j.copsyc.2018.10.013.

Geyer, T., Zehetleitner, M., Müller, H.J., 2010. Contextual cueing of pop-out visual search: When context guides the deployment of attention. Journal of Vision 10, 20. https://doi.org/10.1167/10.5.20.

Guedj, C., Vuilleumier, P., 2020. Functional connectivity fingerprints of the human pulvinar: decoding its role in cognition. Neuroimage 221, 117162. doi:10.1016/j.neuroimage.2020.117162.

Halassa, M.M., Acsády, L., 2016. Thalamic Inhibition: Diverse Sources, Diverse Scales. Trends Neurosci 39, 680–693. https://doi.org/10.1016/j.tins.2016.08.001.

Haxby, J.V., Gobbini, M.I., Furey, M.L., Ishai, A., Schouten, J.L., Pietrini, P., 2001. Distributed and overlapping representations of faces and objects in ventral temporal cortex. Science 293, 2425–2430. doi:10.1126/science.1063736.

Hernández-García, A., Ramos Gameiro, R., Grillini, A., König, P., 2020. Global visual salience of competing stimuli. J. Vis. 20, 27. doi:10.1167/jov.20.7.27.

Kaas, J.H., Lyon, D.C., 2007. Pulvinar contributions to the dorsal and ventral streams of visual processing in primates. Brain Res. Rev. 55, 285–296. doi:10.1016/j.brainresrev.2007.02.008.

Kanwisher, N., McDermott, J., Chun, M.M., 1997. The fusiform face area: a module in human extrastriate cortex specialized for face perception. J. Neurosci. 17, 4302–4311. doi:10.1523/JNEUROSCI.17-11-04302.1997.

Kastner, S., Ungerleider, L.G., 2000. Mechanisms of visual attention in the human cortex. Annu Rev Neurosci 23, 315–341. https://doi.org/10.1146/annurev.neuro.23.1.315.

Kincade, J.M., Abrams, R.A., Astafiev, S.V., Shulman, G.L., Corbetta, M., 2005. An event-related functional magnetic resonance imaging study of voluntary and stimulus-driven orienting of attention. J. Neurosci. 25, 4593–4604. doi:10.1523/JNEUROSCI.0236-05.2005.

Komura, Y., Nikkuni, A., Hirashima, N., Uetake, T., Miyamoto, A., 2013. Responses of pulvinar neurons reflect a subject's confidence in visual categorization. Nat. Neurosci. 16, 749–755. https://doi.org/10.1038/nn.3393.

Krauth, A., Blanc, R., Poveda, A., Jeanmonod, D., Morel, A., Székely, G., 2010. A mean three-dimensional atlas of the human thalamus: generation from multiple histological data. Neuroimage 49, 2053–2062. doi:10.1016/j.neuroimage.2009.10.042.

LaBerge, D., Buchsbaum, M.S., 1990. Positron emission tomographic measurements of pulvinar activity during an attention task. J. Neurosci. 10, 613–619.

Landsheer, J.A., van den Wittenboer, G., 2015. Unbalanced 2 x 2 factorial designs and the interaction effect: a troublesome combination. PLoS One 10, e0121412. doi:10.1371/journal.pone.0121412.

Langton, S.R.H., Law, A.S., Burton, A.M., Schweinberger, S.R., 2008. Attention capture by faces. Cognition 107, 330–342. https://doi.org/10.1016/j.cognition.2007.07.012.

Llano, D.A., 2013. Functional imaging of the thalamus in language. Brain Lang 126, 62–72. https://doi.org/10.1016/j.bandl.2012.06.004.

Lundqvist, D., Flykt, A., Ohman, A., 1998. The Karolinska directed emotional faces. (KDEF). [Database record]. APA PsycTests. https://doi.org/10.1037/t27732-000.

Lucas, N., Bourgeois, A., Carrera, E., Landis, T., Vuilleumier, P., 2019. Impaired visual search with paradoxically increased facilitation by emotional features after unilateral pulvinar damage. Cortex 120, 223–239. https://doi.org/10.1016/j.cortex.2019.06.009.

Lavie, N., Ro, T., Russell, C., 2003. The Role of Perceptual Load in Processing Distractor Faces. Psychol Sci 14, 510–515. https://doi.org/10.1111/1467-9280.03453.

Mesulam, M.M., 1999. Spatial attention and neglect: parietal, frontal and cingulate contributions to the mental representation and attentional targeting of salient extrapersonal events. Phil. Trans. R. Soc. Lond. B 354, 1325–1346. doi:10.1098/rstb.1999.0482.

Müller, N.G., Ebeling, D., 2008. Attention-modulated activity in visual cortex—more than a simple 'spotlight. Neuroimage 40, 818–827. doi:10.1016/j.neuroimage.2007.11.060.
Mumford, J.A., 2012. A power calculation guide for fMRI studies. Soc. Cogn. Affect. Neurosci. 7, 738–742. doi:10.1093/scan/nss059.
Penny, W.D., Stephan, K.E., Daunizeau, J., Rosa, M.J., Friston, K.J., Schofield, T.M., Leff, A.P., 2010. Comparing families of dynamic causal models. PLoS Comput. Biol. 6, e1000709. doi:10.1371/journal.pcbi.1000709.
Petersen, S.E., Posner, M.I., 2012. The attention system of the human brain: 20 years after. Annu. Rev. Neurosci. 35, 73–89. doi:10.1146/annurev-neuro-062111-150525.
Peyrin, C., 2018. ReCor Database.
Posner, M.I., 1980. Orienting of attention. Q J Exp Psychol 32, 3–25.
Posner, M.I., Petersen, S.E., 1990. The attention system of the human brain. Annu. Rev. Neurosci. 13, 25–42. doi:10.1146/annurev.ne.13.030190.000325.
Purushothaman, G., Marion, R., Li, K., Casagrande, V.A., 2012. Gating and control of primary visual cortex by pulvinar. Nat. Neurosci. 15, 905–912. doi:10.1038/nn.3106.
Rafal, R.D., Posner, M.I., 1987. Deficits in human visual spatial attention following thalamic lesions. Proc. Natl. Acad. Sci. U.S.A. 84, 7349–7353. doi:10.1073/pnas.84.20.7349.
Reynaud, A.J., Froesel, M., Guedj, C., Ben Hadj Hassen, S., Cléry, J., Meunier, M., Ben Hamed, S., Hadj-Bouziane, F., 2019. Atomoxetine improves attentional orienting in a predictive context. Neuropharmacology 150, 59–69. doi:10.1016/j.neuropharm.2019.03.012.
Reynolds, J.H., Chelazzi, L., Desimone, R., 1999. Competitive mechanisms subserve attention in macaque areas V2 and V4. J Neurosci 19, 1736–1753.
Rissman, J., Gazzaley, A., D'Esposito, M., 2004. Measuring functional connectivity during distinct stages of a cognitive task. Neuroimage 23, 752–763. doi:10.1016/j.neuroimage.2004.06.035.
Rothman, K.J., 1990. No adjustments are needed for multiple comparisons. Epidemiology 1, 43–46.
Saalmann, Y.B., Ly, R., Pinsk, M.A., Kastner, S., 2018. Pulvinar influences parietal delay activity and information transmission between dorsal and ventral visual cortex in macaques. bioRxiv 405381; doi: https://doi.org/10.1101/405381
Saalmann, Y.B., Kastner, S., 2011. Cognitive and perceptual functions of the visual thalamus. Neuron 71, 209–223. https://doi.org/10.1016/j.neuron.2011.06.027.
Saalmann, Y.B., Pinsk, M.A., Wang, L., Li, X., Kastner, S., 2012. The pulvinar regulates information transmission between cortical areas based on attention demands. Science 337, 753–756. doi:10.1126/science.1223082.
Shipp, S., 2003. The functional logic of cortico-pulvinar connections. Philos. Trans. R. Soc. Lond. B Biol. Sci. 358, 1605–1624. doi:10.1098/rstb.2002.1213.
Silver, M.A., Kastner, S., 2009. Topographic maps in human frontal and parietal cortex. Trends Cogn Sci 13, 488–495. https://doi.org/10.1016/j.tics.2009.08.005.
Snow, J.C., Allen, H.A., Rafal, R.D., Humphreys, G.W., 2009. Impaired attentional selection following lesions to human pulvinar: evidence for homology between human and monkey. Proc. Natl. Acad. Sci. U.S.A. 106, 4054–4059. doi:10.1073/pnas.0810086106.
Somers, D.C., Dale, A.M., Seiffert, A.E., Tootell, R.B., 1999. Functional MRI reveals spatially specific attentional modulation in human primary visual cortex. Proc. Natl. Acad. Sci. U. S. A. 96, 1663–1668. doi:10.1073/pnas.96.4.1663.
Stewart-Oaten, A., 1995. Rules and judgments in statistics: three examples. Ecology 76, 2001–2009. doi:10.2307/1940736.
Vossel, S., Thiel, C.M., Fink, G.R., 2008. Behavioral and neural effects of nicotine on visuospatial attentional reorienting in non-smoking subjects. Neuropsychopharmacology 33, 731–738. doi:10.1038/sj.npp.1301469.
Vossel, S., Weidner, R., Driver, J., Friston, K.J., Fink, G.R., 2012. Deconstructing the Architecture of Dorsal and Ventral Attention Systems with Dynamic Causal Modeling. J. Neurosci. 32, 10637–10648. https://doi.org/10.1523/JNEUROSCI.0414-12.2012.
Vuilleumier, P., Armony, J.L., Driver, J., Dolan, R.J., 2001. Effects of attention and emotion on face processing in the human brain: an event-related fMRI study. Neuron 30, 829–841. doi:10.1016/S0896-6273(01)00328-2.
Wilke, M., Schneider, L., Dominguez-Vargas, A.U., Schmidt-Samoa, C., Miloserdov, K., Nazzal, A., Dechent, P., Cabral-Calderin, Y., Scherberger, H., Kagan, I., Bähr, M., 2018. Reach and grasp deficits following damage to the dorsal pulvinar. Cortex 99, 135–149. doi:10.1016/j.cortex.2017.10.011.
Willenbockel, V., Sadr, J., Fiset, D., Horne, G.O., Gosselin, F., Tanaka, J.W., 2010. Controlling low-level image properties: the SHINE toolbox. Behav. Res. Methods 42, 671–684. doi:10.3758/BRM.42.3.671.
Wolfe, J.M., 2021. Guided search 6.0: an updated model of visual search. Psychon. Bull. Rev. 28, 1060–1092. doi:10.3758/s13423-020-01859-9.
Zeidman, P., Jafarian, A., Corbin, N., Seghier, M.L., Razi, A., Price, C.J., Friston, K.J., 2019a. A guide to group effective connectivity analysis, part 1: first level analysis with DCM for fMRI. Neuroimage 200, 174–190. doi:10.1016/j.neuroimage.2019.06.031.
Zeidman, P., Jafarian, A., Seghier, M.L., Litvak, V., Cagnan, H., Price, C.J., Friston, K.J., 2019b. A guide to group effective connectivity analysis, part 2: second level analysis with PEB. Neuroimage 200, 12–25. doi:10.1016/j.neuroimage.2019.06.032.
Zhou, H., Schafer, R.J., Desimone, R., 2016. Pulvinar-cortex interactions in vision and attention. Neuron 89, 209–220. doi:10.1016/j.neuron.2015.11.034.

Further reading

Gazzaley, A., Cooney, J.W., McEvoy, K., Knight, R.T., D'Esposito, M., 2005. Top-down enhancement and suppression of the magnitude and speed of neural activity. J. Cogn. Neurosci. 17, 507–517. doi:10.1162/0898929053279522.
He, B.J., Snyder, A.Z., Vincent, J.L., Epstein, A., Shulman, G.L., Corbetta, M., 2007. Breakdown of functional connectivity in frontoparietal networks underlies behavioral deficits in spatial neglect. Neuron 53, 905–918. doi:10.1016/j.neuron.2007.02.013.
Hwang, K., Shine, J.M., D'Esposito, M., 2019. Frontoparietal activity interacts with task-evoked changes in functional connectivity. Cereb. Cortex 29, 802–813. doi:10.1093/cercor/bhy011.
Koch, C., Ullman, S., 1985. Shifts in selective visual attention: towards the underlying neural circuitry. Hum. Neurobiol. 4, 219–227.